Microsyst Technol (2015) 21:2155–2163
DOI 10.1007/s00542-014-2311-8

TECHNICAL PAPER

# A novel facile synthesis and electromagnetic wave shielding effectiveness at microwave frequency of graphene oxide paper

**Nadia Abdel Aal · Faten Al-Hazmi · Ahmed A. Al-Ghamdi · Attieh A. Al-Ghamdi · Farid El-Tantawy · F. Yakuphanoglu**

Received: 13 August 2014 / Accepted: 18 August 2014 / Published online: 6 September 2014


**Abstract** Nano-structured graphene oxide (GO) freestanding paper was synthesized by an arc recharge technique in flowing of oxygen for the first time. This technique offers new ways on how e.g. layers structure nanomaterials could be produced. The morphology and structural properties of the as-synthesized GO were examined by means of X-ray diffraction, Fourier transform infrared spectra, scanning electrom microscopy, energy dispersive x-ray spectroscopy, transmission electron microscopy, high resolution transmission electron microscopy and selective area electron diffraction techniques. The structural and morphological characterizations revealed that the synthesized GO were well-defined nanosheets with a thickness of 6 nm. The optical band gap was calculated from the absorption spectrum, and was found to be 3.32 eV. Furthermore, we aim to use GO paper to develop new electromagnetic interference shielding sheets that have a high shielding effectiveness (SE) (over 30 dB) at frequencies in the 1–12 GHz range. The complex permittivity and total shielding effectiveness of as synthesized GO freestanding paper are measured at frequencies from 1 to 12 GHz. Finally, to enhance the performances of the electromagnetic shields effectiveness, five-layered GO sheets were made. Furthermore, the highest SE for the light-weight freestanding GO paper was 50 dB at 1 GHz, indicating commercial use for many industrial or military shielding applications as an attractive candidate for the new type of microwave shielding.

N. A. Aal
Department of Chemistry, Faculty of Science, Suez Canal University, Ismailia, Egypt

F. Al- Hazmi · Ahmed A. Al-Ghamdi
Department of Physics, Faculty of Science, King Abdulaziz University, P. O. 80203, Jeddah 21589, Saudi Arabia

Attieh A. Al-Ghamdi
Center of Nanotechnology, King Abdulaziz University, Jeddah, Saudi Arabia

F. El-Tantawy
Department of Physics, Faculty of Science, Suez Canal University, Ismailia, Egypt

F. Yakuphanoglu (✉)
Department of Physics, Faculty of Science, Firat University, Elazig 23169, Turkey
e-mail: fyhan@hotmail.com

## 1 Introduction

As a new material, graphene is one of the most exciting materials being investigated today and has unusual structure and many unique physical, chemical and mechanical properties (Al-Ghamdi et al. 2014a; Yan et al. 2008). Graphene, a novel single atom thick two-dimensional plane layer of sp2-bonded carbon, is a building block for the formation of 3D graphite, 1D carbon nanotubes, and 0D fullerenes (Maddinedi et al. 2014; Al-Ghamdi et al. 2014b). Generally, graphene oxide (GO) is an atomic sheet of graphite decorated by several oxygenated functional groups on its basal planes and at its edges, resulting in a hybrid structure comprising a mixture of sp2 and sp3 hybridized carbon atoms (Dikin et al. 2007; Bu 2013). Due to its unique structure, GO possesses many desirable properties such as high melting points, good chemical stability, good thermal conductivity, high intrinsic mobility, good electrical conductivity, high optical transparent and extraordinary mechanical properties. These outstanding properties make GO quite attractive for standalone applications in various fields such as optoelectronics, supercapacitors, memory devices, composite materials,

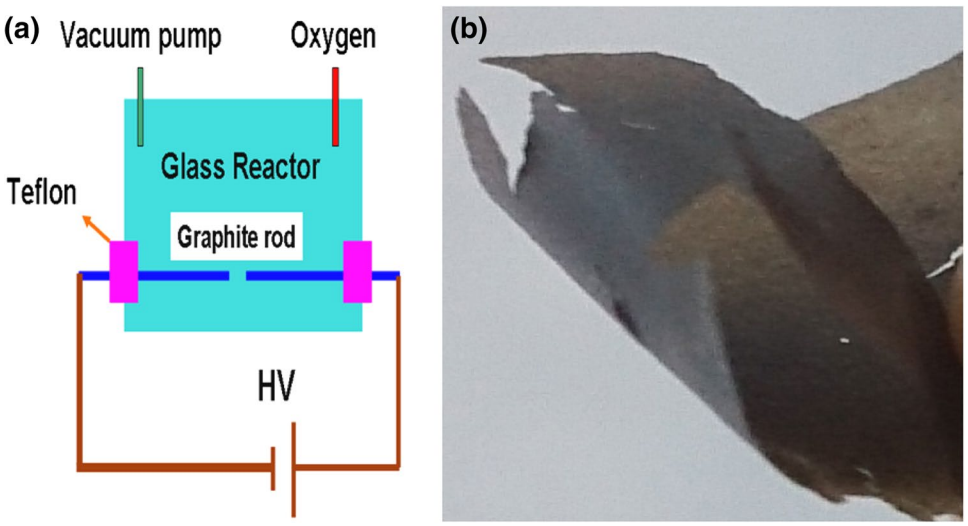


**Fig. 1** **a** Schematic diagram of arc discharge technique to prepare GO nanosheets and **b** photographic image of GO freestanding paper

photocatalysis, drug delivery agent, among many other potential applications (Lou et al. 2014; Wang et al. 2008). In fact, GO is generally synthesized through the oxidation of graphite using strong oxidizers following the exfoliation of this graphitic oxide into graphene oxide that occurs by either thermal treatment or ultrasonic process (Al-Ghamdi et al. 2014c; Singh et al. 2011). Thereat, the synthesis of GO by chemical methods is very expensive, long time, partial oxidation and agglomeration of graphene always limited its applications. Therefore, it is urgent to explore new method of synthesize GO in large scale with low cost. This has drawn the uncountable attention of researchers to explore the intriguing properties and applications of GO nanoparticles.

Currently, the electromagnetic wave in the GHz ranges has been widely applied in both commercial and military field such as wireless telecommunication systems, radar, local area network, etc. and caused electromagnetic interference (Karthikeyan Krishnamoorthy et al. 2013; Rodríguez-González et al. 2014). In fact, the electromagnetic waves emitted by electronic devices can also reveal sensitive information about the device to the environment, termed electromagnetic information leakage. Furthermore, the emerging hazards of microwave frequency on electrical and electronic devices performance and human health have attracted considerable attention in all modern society. Conventionally, metal and conducting ceramic sheeting are commonly used to solve these problems but seams commonly encountered because are typically heavy, expensive, suffer corrosion, cause some radiation leakage and diminish the effectiveness of shielding. Therefore, a new material is needed to overcome these problems. To solve the problems of electromagnetic interference and information leakage, needless electromagnetic wave emission must be decreased.

The first purpose of this study is to explore a new, fast and efficient methods of synthesis high purity GO in large scale with low cost by arc recharge method. The microstructure and optical properties of the GO was systematically investigated by characterization techniques. The second aim is focusing on the applicability of synthesized GO freestanding paper for electromagnetic shielding effectiveness (SE) over the microwave range of 1–12 GHz. The effect of sample thickness on SE has also been examined.

## 2 Experimental details

### 2.1 Synthesis of GO freestanding paper nanosheets

Graphene oxide (GO) was synthesized from graphite rods using arc reactor technique as follows. The arc reactor consisted of anode graphite rod (5 mm diameter, 200 mm length). The cathode, a pure graphite rod of 5 mm diameter, was horizontally fixed by a stationary holder. The arc reactor was first evacuated. With the anode tip gradually being moved toward the cathode, an arc-discharge process was maintained between the tips of the anode and the cathode. The arc-discharge was generated by an approximate 50 kV and a DC current from the range of 25 A. The arc gap between the electrodes was kept in 1 mm distance, by manually advancing the consumed anode. The dynamic flowing of oxygen gas was supplied in the pressure of 260 Torr and at a flow rate of 5–10 L/min. The duration of the arc-discharge process was about 2 s. After the arc process a large quantities of cotton-like graphite soot namely graphene oxide (GO) attached on the chamber walls. A typical schematic of arc-discharge technique to prepare GO nanosheets is shown in Fig. 1a. Colloidal dispersions of as synthesized individual graphene oxide in water at the concentration of

5 mg $ml^{-1}$ were prepared with the aid of magnetic stirring for 1 h. GO freestanding paper was made by filtration of the resulting colloid through a commercial membrane filter paper (25 mm in diameter, 0.1 mm pore size; Whatman), followed by air drying and peeling from the filter. The photographic image of GO free standing paper is shown in Fig. 1b. The thickness of each GO freestanding paper sample was controlled by adjusting the volume of the colloidal suspension. Samples of GO freestanding paper prepared in this manner were cut by a razor blade into rectangular strips of approximately 5 mm × 330 mm for testing without further modification.

### 2.2 Characterization of as-synthesized GO nanosheets

The as-synthesized GO freestanding paper were characterized in detail by various analytical tools. The crystal phases of the pristine graphite and prepared GO were examined by X-ray diffraction (X-ray; PANanalytical Xpert Pro.) pattern measured with $Cu - k\alpha$ radiation ($\lambda = 0.154178$ nm) operating at 20 keV and 40 mA. The diffraction data were collected automatically at room temperature in the angular range of $5° \leq 2\theta \leq 80°$ with the step width of 0.05° and scan rate of 0.2 s every step.

The chemical composition of the as synthesized GO nanosheets were investigated by Fourier transform infrared spectroscopy (FTIR) measured at room temperature using Nicolet iD5 spectrophotometer in the range of 4,000–500 $cm^{-1}$. The details morphologies of as synthesized GO were conducted by a field emission scanning electron microscopy (FESEM; JEOL-JSM-7600F) equipped with energy dispersive spectroscopy (EDS) and transmission electron microscopy (TEM; Hitachi-H-7500). For detailed structural characterizations of the grown GO nanosheets, high-resolution transmission electron microscopy (HRTEM) equipped with the selected area electron diffraction (SAED) pattern was used. For HRTEM analysis, the synthesized products were ultrasonically dispersed in acetone and a drop of acetone solution, which contains the GO nanostructures, was placed on a copper grid and examined. Room-temperature UV–Vis. spectroscopy was done to examine the optical properties of synthesized GO nanoparticles. The electrical conductivity test was performed on GO samples by means of the standard digital four-point probe system. The dielectric constant was estimated via a Hewlett-Packard impedance analyzer in the frequency ranges of 1–12 GHz. The Hewlett–Packard waveguide line containing spectro-analyzer, power matter, coefficient of reflection meter, and coefficient of attenuation meter determined the electromagnetic interference shielding properties. The measurements were carried out in the frequency ranges of 1–12 GHz.

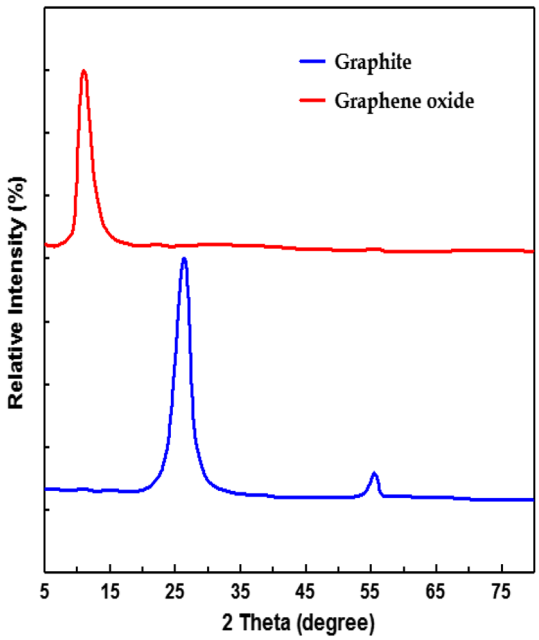


**Fig. 2** X-ray spectra of green graphite and graphene oxide freestanding paper

## 3 Results and discussion

### 3.1 Structural, morphological and optical properties of GO nanosheets

Prior to any applications, the structural, morphological and compositional properties of synthesized GO freestanding paper nanosheets are essential. To examine the crystal structure and particle size, the pristine graphite (G) and prepared graphene oxide (GO) nanoparticles were examined by X-ray powder diffraction. Figure 2 displays the typical X-ray pattern of pristine graphite and synthesized graphene oxide freestanding paper nanoparticles. It is obvious that the reflection peaks at $2\theta = 26.6°$ (002) and $2\theta = 54.8°$ (004) can be unambiguously indexed to the pristine graphite that has an interlayer distance ($d_{002}$) of 0.335 nm, which are in good agreement with JCPDS card (JCPDS 73-1962).

In the X-ray pattern of GO, the strong and sharp peak located at $2\theta = 11.2°$ (002) is a typical diffraction peak of GO, which is attributed to a conserved graphene-like honey comb lattice in graphite oxides, which are in very well agreement with the corresponding bulk values reported for GO structures (Al-Ghamdi et al. 2014a, c). Meanwhile, the observed interlayer spacing ($d_{002}$) of as synthesized GO of about 0.75 nm which corresponds to the GO (Lou et al. 2014). Importantly, the increase in the interlayer space of GO is mainly ascribed to trapping of oxygen atoms and intercalated $H_2O$ molecules will attached to the graphite

lattice and the atomic scale roughness arising from structural defects (sp3 bonding) generated on the originally atomically flat graphene sheet (Al-Ghamdi et al. 2012; Liy and Oya 2014). To sum up, the X-ray results of the GO nanosheets are in good agreement with published reports available in the literatures (Panwar et al. 2012). Meanwhile, the thickness of crystallite ($D_{002}$) of GO was determined by fitting the width of (002) reflection peak using the Debye-Scherer's, which is expressed by (Mahapatra et al. 2008):

$$D_{002} = \left(\frac{k\,\lambda}{\beta\cos\theta}\right) \quad (1)$$

where λ is the X-ray wavelength, $\beta$ is the full width at half-maximum in radian of [002] peak of X-ray pattern and $\theta$ is the Bragg's angle.

The thickness of crystallite GO nanosheets was found to be about 6 nm.

To further characterize the chemical composition and functional groups formed in the synthesized GO the FTIR spectroscopy analysis were done. The typical FTIR spectra of GO freestanding paper are displayed in Fig. 3. Several well defined absorption peaks at 685, 882, 1,040, 1,150, 1,626, 1,718 and 3,330 $cm^{-1}$ are seen in the observed spectrum. The appearance of prominent peaks at around 685 and 882 $cm^{-1}$ coincide with the C–O–C stretching modes of the hexagonal crystal phase clearly confirms the formation of GO. The peak at 1,040 $cm^{-1}$ is concerned to C–O stretching, confirming the presence of oxide functional groups (Koysuren et al. 2008). The peak appeared at 1,150 $cm^{-1}$ is assigned to the O–H deformation vibration. The origination of peak at 1,626 $cm^{-1}$ is a resonance peak that can be assigned to the C–C stretching and absorbed hydroxyl groups in the GO, but may also contain components from the skeletal vibrations of un-oxidized graphitic domains (Wang et al. 2008; Al-Ghamdi et al. 2014c). The adsorption band appeared at 1,718 $cm^{-1}$ is assigned to C=O stretching vibration of the carboxylic COOH groups and C=C stretching mode of the $sp^2$ network (Bu 2013; Lou et al. 2014). Further, spectrum of GO exhibits a broad signal at 3,330 $cm^{-1}$ regime is attributed to the surface O–H stretching vibrations and intercalated free $H_2O$ molecules. The observed FTIR results are well matched with already reported literatures (Dikin et al. 2007; Bu 2013; Lou et al. 2014; Wang et al. 2008).

The general morphologies of as synthesized GO freestanding paper nanosheets were fully analyzed through FESEM, TEM and HRTEM observations. The FESEM micrograph of GO is displayed in Fig. 4a. It is apparent that the synthesized GO nanosheets possess a homogeneous surface sheet like morphology (i.e. layered stacked structure) with the characteristics wrinkles and ripples of

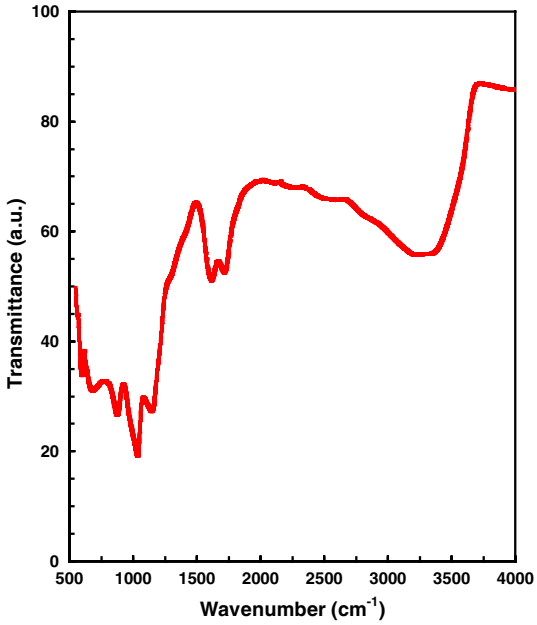


**Fig. 3** FTIR spectra of as prepared GO freestanding paper

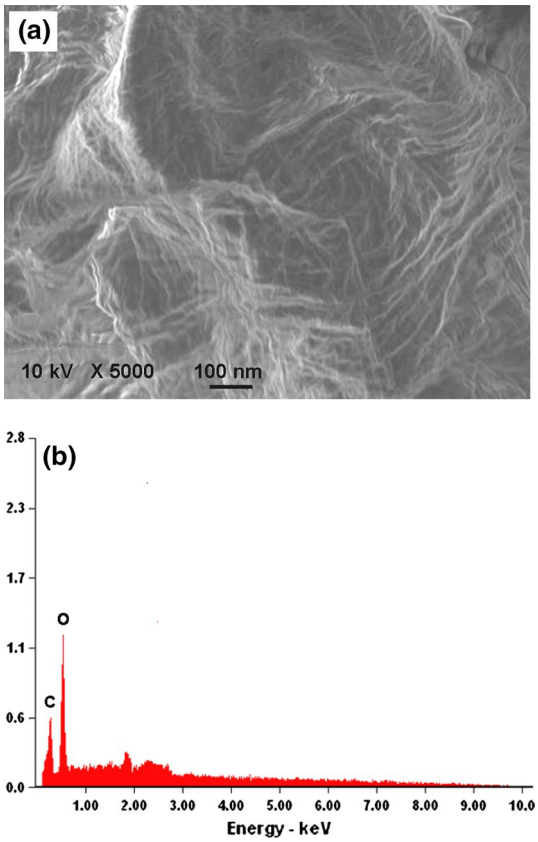


**Fig. 4** Typical **a** FESEM images and **b** EDS spectrum of prepared GO nanoparticles

graphene 2D structure. Furthermore, the sheets display layers with different transparencies and grown in large scale. This is probably due to the number of layers present in the stacked structure of GO (Bu 2013). The typical thicknesses of the synthesized GO nanosheets are in the range of 7 nm with several micrometers in width.

To check the elemental composition of as synthesized GO nanosheets, energy dispersive spectroscopy (EDS) is done and depicted in Fig. 4b. It is clear from the EDS spectrum that the synthesized GO are made of carbon (C) and oxygen. No peak linked with any other impurity has been noticed in the spectrum, up to the detection limit of EDS instrument and thus, again substantiate that the synthesized products are pure GO formed by carbon and oxygen.

Figure 5a exhibits the typical low-resolution TEM image of the as-synthesized GO nanosheets. Significantly, the nanostructures are thin nanosheets which are rippled in shape and they resemble crumpled silk veil waves. They are transparent and exhibit a very stable nature under the electron beam. Multilayer GO nanosheets are scrolled and corrugated together with sizes in the range of tens to several hundreds of square nanometers. Fascinatingly, the GO nanosheets are entangled with each other in such a manner that they made well perfect sheet-like morphologies and hence possess larger surface area. All the TEM observations regarding shape, size and thickness are fully consistent with the obtained X-ray and FESEM results and confirmed that the synthesized GO are thin nanosheets of large lateral dimensions, rippled and transparent with the typical thickness of 6 nm. Therefore, GO nanosheets are promising candidates for modern optoelectronic applications such as gas sensing, photocatlysts, chemical filters, microwave shielding, cellular images and more (Dikin et al. 2007; Bu 2013).

In order to gain more specific details on the surface morphology and crystalline nature of the synthesized GO was realized using HRTEM and selected area electron diffraction (SAED) as shown in Fig. 5b. The ordered graphitic lattices are clearly visible. The observed HRTEM exhibits a very clear and well-defined lattice fringes with the lattice spacing of 0.75 nm, which can be assigned to the (002) crystalline plane of GO (Al-Ghamdi et al. 2014c). The obtained HRTEM results are well matched with the X-ray results.

Selected area electron diffraction further confirmed the ordered or crystalline nature of the GO nanosheets. The SAED pattern is shown as the inset in Fig. 5b. It is clearly seen that the SAED pattern of GO exhibits well-defined diffraction spots with a six-fold pattern unambiguously indicating that the crystalline structure of the GO nanosheets and that is consistent with the hexagonal lattice. This result is in agreement with the microstructure observations mentioned above.

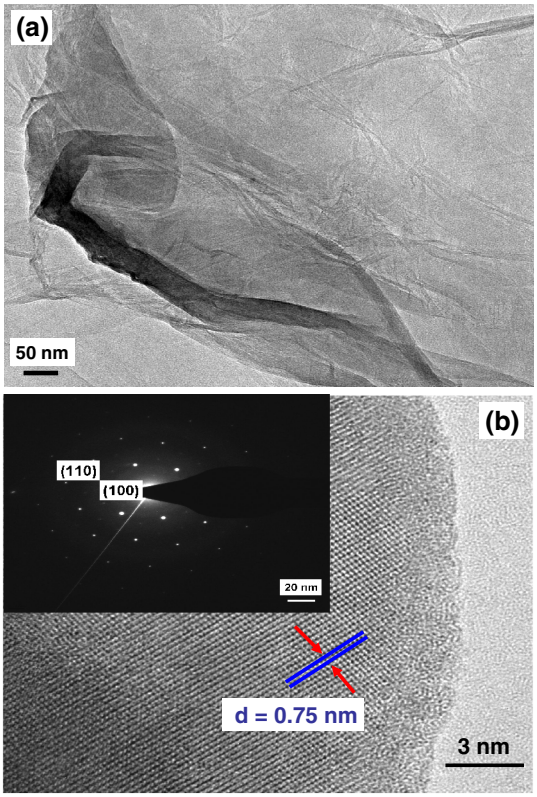


**Fig. 5** **a** TEM image of GO **b** HTTEM image of GO and the inset is electron diffraction patterns of GO sheets

The optical properties are very important parameter to select the materials for use in a particular application. Optical properties of GO freestanding paper were performed using UV–visible spectroscopy. The absorption spectrum of synthesized GO at room temperature is displayed in Fig. 6a. The maximum absorption peak at around 226 nm is observed which is characteristic of $\pi$–$\pi^*$ transition of C=C aromatic bonds and a shoulder at about 302 nm is attributed to n–$\pi^*$ transitions of C–O bonds, which confirms the formation of GO (Al-Ghamdi et al. 2014a; Yan et al. 2008). No other peak, except well-defined absorption peak at 226 nm is observed in the spectrum which confirms that the as synthesized sheet-shaped GO nanostructures are pure and possessing good optical properties.

The optical band gap energy $\left(E_g^{opt}\right)$ is defined by the Tauc's relation (Yan et al. 2008; Maddinedi et al. 2014):

$$\alpha h\upsilon = B\left(h\upsilon - E_g^{opt}\right)^n \tag{2}$$

where $\alpha$ is the absorption coefficient, $h\upsilon$ is the photon energy, $B$ is a constant and $n$ is the parameter which determines the optical transition type and has values $1/2$ and $3/2$ for the direct allowed and forbidden transitions, respectively.

To evaluate the optical band gap energy of the as-synthesized GO, a plot for $(\alpha h\upsilon)^2$, versus $h\upsilon$ has been drawn and results are demonstrate in Fig. 6b. The value of the direct band gap energy was obtained from the linear portion of the plots after extrapolating to zero as shown in Fig. 6b. The linear nature of the plot at the absorption edge confirms that the investigated GO freestanding paper has direct band gap where $E_g^{opt} = 3.32$ eV. The obtained optical band gap is almost similar to the bulk GO and consistent with the reported literature (Al-Ghamdi et al. 2014c; Singh et al. 2011).

### 3.2 Electromagnetic wave shielding performance

The shielding effectiveness (SE) is the ratio of the electromagnetic power density transmitted at point when the sample shield is installed ($P_t$) to the electromagnetic power density incident at the same point before the sample shield is installed ($P_i$):

$$\mathrm{SE} = 10 \log_{10} \left( \frac{P_t}{P_i} \right) \tag{3}$$

SE is the sum of three general mechanisms for electromagnetic shielding (EMS), reflection, absorption and multi-reflection. If the multiple reflections are ignored, the total SE of electo-conductive GO paper is defined and calculated based on the Simon formalism (Al-Ghamdi et al. 2014c; Singh et al. 2011; Karthikeyan Krishnamoorthy et al. 2013).

$$\mathrm{SE} = \left( \frac{P_t}{P_i} \right) = R + A + B \tag{4}$$

where $R$ is the reflection loss, $A$ is the absorption loss and $B$ is the internal re-reflection loss.

The reflection loss is given by equation (Dikin et al. 2007; Bu 2013):

$$R = 168 + \log \left( \frac{f \mu_r}{\sigma_r} \right) \tag{5}$$

The absorption loss ($A$) is given by equation:

$$A = 1.314\, t \sqrt{f \mu_r \sigma_r} \tag{6}$$

where $\mu_r$ is permeability relative to that of copper at the frequency $f$ (H/m), $\sigma_r$ is conductivity relative to that of copper, (conductivity of copper is $5.8 \times 10^{-7}\ \Omega/m$) and $t$ is the thickness of shielding material.

Normally, the shielding effectiveness of a material increases with an increase in frequency. Consequently, high frequency electromagnetic waves only penetrate the near surface region of a shielding material. This is called the skin effect. The skin effect is characterized by skin depth ($\delta$). This is defined as the depth at which the field drops to 1/e of the incident value and is defined by equation (Rodríguez-González et al. 2014; Al-Ghamdi et al. 2014d):

$$\delta = \frac{1}{\sqrt{\pi f \mu_r \sigma_r}} \tag{7}$$

Based on the theory of electromagnetic interference shielding, the SE increases with increasing conductivity of the material. Shielding effectiveness capacity and conductivity are related by the following equation (Rodríguez-González et al. 2014; Al-Ghamdi et al. 2014d):

$$\mathrm{SE} = 20 \log \left(1 + \sigma d Z_0/2\right) \tag{8}$$

where $\sigma$ is the conductivity, $d$ is thickness of the sample, and $Z_0$ is the free space wave impedance (377 Ω).

The electrical conductivity of as synthesized GO paper of about $1.26 \times 10^{-2} (\Omega \mathrm{cm})^{-1}$. It is obvious that SE capacity of the GO paper is about 40 dB at 1 GHz, this is attributed to the formation of conducting networks entire GO structure.

Figure 7 displays the dependence of SE on the frequency for GO freestanding paper. The figure show that the SE decreases with increasing frequency. This can be explained on the basis of formation of conductive network entire the GO structure and high aspect ratio of GO. The frequency dependence of the EMI effect is due to several factors. All three mechanisms of EMI shielding, namely scattering/reflection, absorption, and multiple reflections, are related to frequency and materials size. On the other hand, higher electrical conductivity will result in better EMI shielding because of the reflection effect, in which mobile charge carriers (electrons or holes) and/or delocalized charge displacement are required for interaction with the incident electromagnetic field.

The results of calculated SE of GO paper based on Eqs. 5 and 6 are displayed in Fig. 7. A good agreement is obtained between the measured and the calculated SE in the microwave frequencies.

In fact, the phenomenon of EMI shielding in materials is dependent on the operating variables such as frequency, sample thickness and dimensions. The effect of sample thickness on SE of GO has also been studied. Figure 8 depicts the SE versus GO paper thickness measures at 1 GHz. From the figure it has been observed that SE increase continuously with thickness. This can be explained as follows. The increase in thickness of the sample places more amount of conducting mesh and interception of individual conducting layers, which causes both absorption and internal reflection; thereby SE increases with thickness. Furthermore, because GO papers have high electrical conductivity and large aspect ratio to cover broad length scales, interactions between GO network and ` wave may be less sensitive to frequency. Increase in thickness enhances both

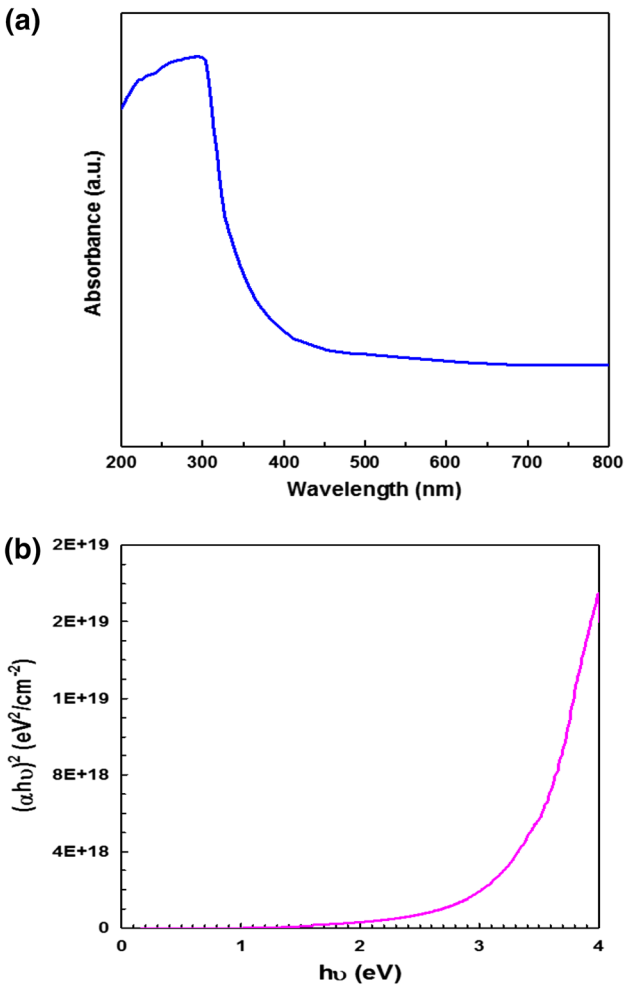


**Fig. 6** **a** The UV–vis spectrum of graphene oxide (GO) free-standing paper and **b** evolution of $(\alpha h\upsilon)^2$ plotted against photon energy $(h\upsilon)$ of GO

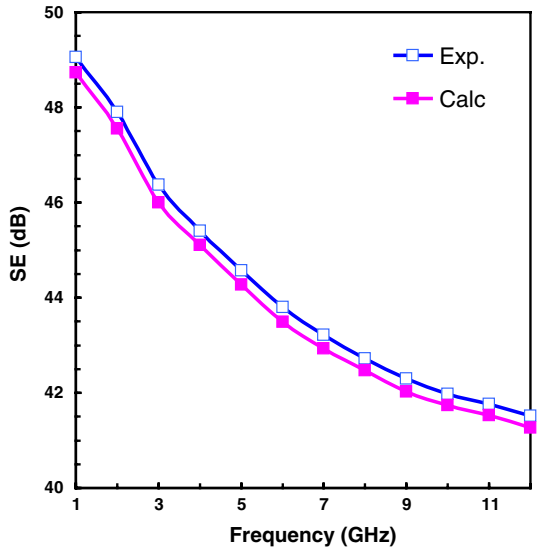


**Fig. 7** EMI shielding effectiveness as a function of frequency measured and calculated in the 1–12 GHz range for GO freestanding paper

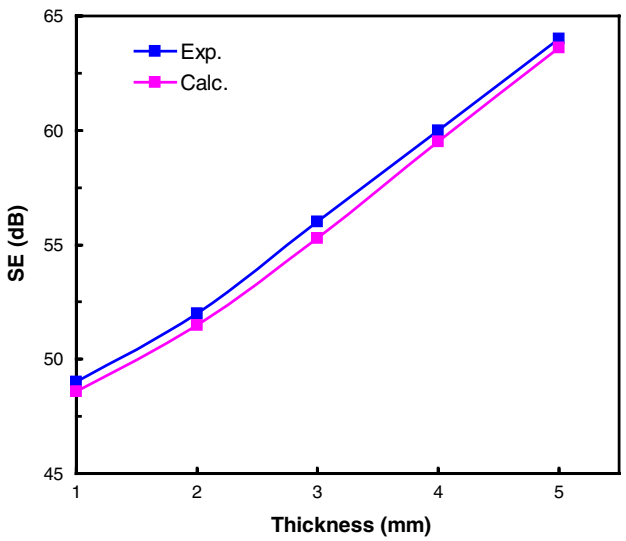


**Fig. 8** Experimental and theoretical data of SE as a function of GO sample thickness at 1 GHz frequency

absorption and multiple internal reflections, leading in higher SE.

For any system possesses a frequency dependent complex dielectric permittivity ($\varepsilon^*$) is determined using the following equation (Bai et al. 2011):

$$\varepsilon^*(\omega) = \varepsilon'(\omega) - i\varepsilon''(\omega) \tag{9}$$

where $\varepsilon'$ represents the relative dielectric constant, $\varepsilon''$ is the imaginary part accounts for the dielectric loss, $i$ denotes the square root of $-1$ and $\omega$ is the angular frequency. The ratio of the imaginary to the real part $\varepsilon''(\omega)/\varepsilon'(\omega)$ is the dissipation factor, which is represented bytan $\delta$, where $\delta$ is called as the loss angle denoting the angle between the voltage and the charging current and can be expressed using the following equation:

$$\tan\delta = \frac{\varepsilon''}{\varepsilon'} = \frac{\sigma}{2\pi f\varepsilon'\varepsilon_0} \tag{10}$$

where $\sigma$ s is the electric conductivity, $f$ is frequency, and $\varepsilon_0$ is the permittivity of the free space $\left(8.85 \times 10^{-12}\ \text{F/m}\right)$.

Therefore, the dielectric property such as the dielectric constant, dielectric loss and loss factor (tan $\delta$) is as important as the EMI shielding effectiveness of electronic and electrical devices because an incident electric field from any source will affect the operational performances of this equipment. The dielectric constant, dielectric loss and dielectric loss factor (tan $\delta$) of GO paper were measured in the frequency range of 1–12 GHz as shown in Fig. 9. As far as we have known, the dielectric property value depends on the number

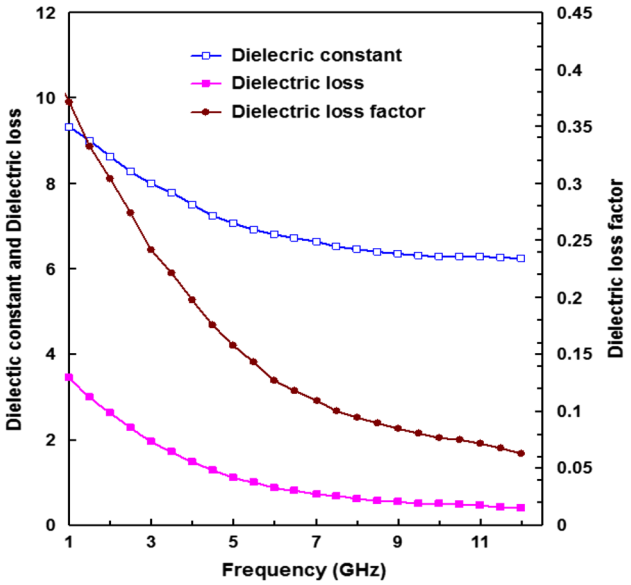


**Fig. 9** Dielectric constant and imaginary dielectric constant as a function of microwave frequency for GO freestanding paper

of mobile charge carriers entire the materials. It is clearly seen that as the frequency increases from 1 to 12 GHz, there is a gradual decrease in $\varepsilon$, $\varepsilon''$ and $\tan\delta$. This can be explained on the electron hopping mode of conduction, which becomes more significant at microwave frequencies, thereby adding to the conductivity already existing, which is reflected in the continuous decrease of $\varepsilon$ and $\varepsilon''$ with increase in frequency. Moreover, the decreases of $\varepsilon$ and $\varepsilon''$ with increasing frequency can also be explained on the basis of frequency dependent relaxation phenomenon of GO structure. Mobile charges form dipoles against the incident electric field. Meanwhile, at a high microwave frequency, mobile charges do not have sufficient time to form dipoles and to absorb the energy of the incident electric field, which might result in low dielectric constant values (Koysuren et al. 2008).

It is well known that, the dielectric loss factor ($\tan\delta$) indicates the inherent dissipation of electromagnetic energy for dielectric materials. The frequency dependency of $\tan\delta$ of GO paper is displayed in Fig. 9. It is obvious that the $\tan\delta$ decreased with increasing frequency. This can be attributed to the resonance behavior. Such resonance may be due to the reorientation of bound charges in the system or its rotational degrees of freedom (Yan et al. 2008; Maddinedi et al. 2014).

## 4 Conclusions

A novel graphene oxide freestanding paper was successfully synthesized with low cost approach and scalable for the first time using arc-recharge technique. This technique opens up new alternative avenues to the conventional chemical reduction methods and makes a potential contribution to the application of GO-based freestanding paper in coming future an exciting materials in optoelectronic components and structural composite. The formation of GO was confirmed through X-ray, FTIR and UV–vis analysis. The X-ray results revealed that the formations of highly crystalline GO. The morphological observations showed a sheet like morphology with thickness of about 6 nm naturally corrugated into ripples like wavy silk. The UV absorption spectra showed an absorption peak at 226 nm which is characteristic of $\pi$–$\pi^*$ transition of C=C aromatic bonds and a shoulder at about 302 nm is attributed to $n$–$\pi^*$ transitions of C–O bonds, which confirms the formation of GO. The optical band gap of GO nanosheets is about 3.32 eV. The experimentally determined SE of the GO paper is about 50 dB at 1 GHz and about 42 dB at 12 GHz, showing a great potential to be used in the field of protecting people from electromagnetic wave and electronic devices at microwave frequency. Finally, the SE is highly enhanced with increasing thickness of light weight GO paper and attained about 70 dB and is therefore compatible with aeronautical applications. The dielectric properties of GO paper are enhanced over microwave frequency.

**Acknowledgments** Authors gratefully acknowledge and thank the Deanship of Scientific Research, King Abdulaziz University (KAU), Jeddah, Saudi Arabia, for the research group "Advances in composites, Synthesis and applications". This work is as a result of international collaboration of the group with Prof. F. Yakuphanoglu. Also, Prof. Dr. Farid El-Tantawy thanks to TUBITAK, Turkey for financial supporting under 2221-Fellowships for Visiting Scientists and Scientists on Sabbatical.

## References

Al-Ghamdi A, Al-Hartomy OA, Al-Salamy F, Al-Ghamdi AA, El-Mossalamy EH, Abdel Daiem AM, Farid El-Tantawy (2012) Novel electromagnetic interference shielding effectiveness in the microwave band of magnetic nitrile butadiene rubber/magnetite nanocomposites. J Appl Polymer Sci 125:2604–2613

Al-Ghamdi A, Al-Hartomy OA, El-Tantawy F, Yakuphanoglu F (2014a) Novel polyvinyl alcohol/silver hybrid nanocomposites for high performance electromagnetic wave shielding effectiveness. Microsyst Technol doi:10.1007/s00542-014-2120-0

Al-Ghamdi AA, Al-Hartomy Omar A, El Okr M, Nawar AM, El-Gazzar S, El-Tantawy F, Yakuphanoglu F (2014b) Semiconducting properties of Al doped ZnO thin films. Spectrochim Acta Part A: Mol Biomol Spectrosc 131:512–517

Al-Ghamdi AA, Al-Hartomy OA, Al-Solamy F, Al-Ghamdi AA, Nikolay D, El-Mossalamy EH, El-Tantawy F (2014c) Dielectric and microwave properties of polyvinyl chloride/graphite/nickel composites and its applications. J Thermoplast Compost Mater 27(4):528–540

Al-Ghamdi A, Al-Hartomy OA, Al-Solamy F, Faten Al-Hazmi, Attieh Al-Ghamdi A, El-Mossalamy EH, Farid El-Tantawy (2014d) On

the prospects of conducting polyaniline/natural rubber composites for electromagnetic shielding effectiveness applications. J Thermoplast Compost Mater 27(6):765–782

Bai Xin, Zhai Yinghao, Zhang Yong (2011) Green approach to prepare graphene-based composites with high microwave absorption capacity. J Phys Chem C 115:11673–11677

Bu Ian YY (2013) Highly conductive and transparent reduced graphene oxide/aluminium doped zinc oxide nanocomposite for the next generation solar cell applications). Opt Mater 36:299–303

Dikin Dmitriy A, Stankovich Sasha, Zimney Eric J, Piner Richard D, Dommett GHB, Evmenenko Guennadi, Nguyen SonBinh T, Ruoff Rodney S (2007) Preparation and characterization of graphene oxide paper. Nature 448:457–460

Karthikeyan Krishnamoorthy A, Murugan Veerapandian B, Kyusik Yun B, Kim S-J (2013) The chemical and structural analysis of graphene oxide with different degrees of oxidation. Carbon 53:38–49

Koysuren Ozcan, Yesil Sertan, Bayram Goknur, Secmen Mustafa, Civi Ozlem Aydin (2008) Effect of a carbon black surface treatment on the microwave properties of poly(ethylene terephthalate)/carbon black composites. J Appl Polym Sci 109:152–159

Liy BoJue, Oya Takahide (2014) Fabrication of novel electromagnetic shielding sheets using carbon-nanotube-composite paper. J Surf Sci Nanotechnol 12:242–246

Lou Yueyun, Liu Gongping, Liu Sainan, Shen Jie, Jin Wanqin (2014) A facile way to prepare ceramic-supported graphene oxide composite membrane via silane-graft modification. Appl Surf Sci 307:631–637

Maddinedi SB, Mandal BK, Vankayala R, Kalluru P (2014) Casein mediated green synthesis and decoration of reduced graphene oxide. Spectrochim Acta Part A: Mol Biomol Spectrosc 126 227–231

Mahapatra SP, Sridhar V, Tripathy DK (2008) Impedance analysis and electromagnetic interference shielding effectiveness of conductive carbon black reinforced microcellular epdm rubber vulcanizates. Polym Compos 10:465–472

Panwar Varij, Mehra RM, Park Jong-Oh, Park Suk-ho (2012) Dielectric analysis of high-density polyethylene-graphite composites for capacitor and emi shielding application. J Appl Polym Sci 125:E610–E619

Rodríguez-González C, Cid-Luna HE, Salas P, Castaño VM (2014) Hydroxyapatite-functionalized graphene: a new hybrid nanomaterial. J Nanomater Article ID 940903, Vol 7

Singh AP, Mishra M, Chandra A, Dhawan SK (2011) Graphene oxide/ferrofluid/cement composites for electromagnetic interference shielding application. Nanotechnology 22

Wang Guoxiu, Yang Juan, Park Jinsoo, Gou Xinglong, Wang Bei, Liu Hao, Yao Jane (2008) Facile synthesis and characterization of graphene nanosheets. J Phys Chem C 112:8192–8195

Yan Zhang, Zhuxia Zhang, Tianbao Li, Xuguang Liu (2008) Xu Bingshe (2008) XPS and XRD study of $FeCl_3$–graphite intercalation compounds prepared by arc discharge in aqueous solution. Spectrochim Acta Part A: Mol Biomol Spectrosc 70(5):1060–1106